Study of hyperfine interactions in charged-particle beams (a review of experimental methods)

A. Hrynkiewicz

Nuclear Physics Institute, Kraków

Fiz. Elem. Chastits At. Yadra 9, 903–937 (July–August 1978)

The article reviews methods of investigation of hyperfine interactions in beams of charged particles. Individual methods are illustrated by examples of their application. Fields of nuclear and solid state physics in which use of the methods described is particularly promising are also discussed.

PACS numbers: 25.90. + k, 34.90. + q

INTRODUCTION

Beams of charged particles from accelerators are used to study hyperfine interactions in *near-beam* experiments by means of installations such as ISOLDE in which short-lived radioactive nuclides located far from the β-stability line are obtained and separated in a mass separator and then studied by the methods of nuclear spectroscopy, and in *in-beam* experiments in which direct use is made of the orientation of the nuclides produced in a nuclear reaction and their recoil velocity. The present article is devoted to these experiments.

Experiments carried out in beams of charged particles, particularly in beams of heavy ions, permit the study of hyperfine interactions of highly excited nuclear states which are inaccessible in radioactive-decay processes and also states with large angular momentum transferred by the bombarding particles.

The large electric charge carried by the heavy ion into the target region adjacent to the nucleus permits investigation of states obtained as the result of multiple Coulomb excitation, and also measurement of the electric quadrupole moments of excited states of nuclei by the reorientation method.

The development of new methods and the refinement of already existing methods of investigating hyperfine interactions has significantly extended the range of lifetimes of nuclear states for which measurements are carried out. On the one hand, with use of transient magnetic fields acting on nuclei moving in a magnetized ferromagnet, measurements are made for states with lifetimes less than 1 psec, and on the other hand, by combining the nuclear magnetic resonance method in the beam with detection of nuclear radiation, hyperfine interactions of states with lifetimes greater than 1 sec are studied.

The hyperfine interaction is studied in two forms. By studying the behavior of nuclei in a known electromagnetic environment, their magnetic dipole and electric quadrupole moments are determined. On the other hand, with use of a nucleus in a state with known angular momenta it is possible to obtain data on the microscopic electromagnetic structure and dynamics of a given material.

The scientific significance of investigations of condensed media by the study of hyperfine interactions is increasing rapidly. The determination of internal magnetic fields and electric field gradients, and also their time dependence, provides unique information on the behavior of impurity atoms implanted in various lattices, on the nature and dynamics of radiation damage, etc. In the study of hyperfine interactions in highly ionized atoms moving in vacuum or a gas it is possible to obtain information on unusual states of the electron shell.

In nuclear reactions it is possible to produce isomeric states of almost all elements over a wide range of lifetimes. Thus, for a given problem it is easy to choose the appropriate nuclear probe and a suitable time scale.

The startup of the new multiply charged ion accelerators will extend still further the arsenal of isomeric states which can be used to study solids, and also will permit production of nuclear states of new types which will be of special interest for nuclear theory. Reactions induced by multiply charged ions, as a result of the large number of possible channels, large transferred angular momentum, and high recoil energy will undoubtedly play a special role in the study of hyperfine interactions in-beam.

1. FEATURES OF REACTIONS INDUCED BY MULTIPLY CHARGED IONS

Nuclear states excited in reactions induced by multiply charged ions. The principal process of interaction of a multiply charged ion with a target nucleus in the case of a limiting bombarding-ion energy below the Coulomb barrier is Coulomb excitation of the nucleus. With increase of the mass of the incident particle, the probability of multiple excitation increases (Fig. 1), which permits production of nuclear states with large angular momentum. In the region of deformed nuclei it is possible in this way to excite states of a rotational band with spin I greater than 30.

At energies above the Coulomb barrier the principal role is played by fusion reactions (HI, xn), which lead to formation of a neutron-deficient final nucleus, and deep inelastic reactions, which involve transfer of many nucleons, in which both nuetron-deficient and neutron-rich final nuclei are formed.

To create a compound nucleus it is necessary that the

 0090-4759/78/040360-13$02.80

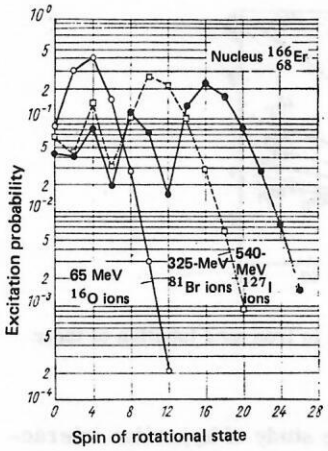

FIG. 1. Probability of multiple Coulomb excitation of rotational states of ^{166}Er by means of multiply charged ions.

orbital angular momentum of the projectile-target system not exceed a critical value l_{crit}. However, the values of l_{crit} lie rather high, so that, for example, a compound nucleus with $Z=80$ can be produced in an excited state with spin of about 90. Transition from a high-spin state to the yrast line occurs with emission first of several neutrons and then a cascade of γ rays with multipolarity not exceeding two. The ground-state band is reached in the course of several picoseconds from the moment of creation of the compound nucleus.

Nuclear orientation of reaction products. In principle all reaction products with spin $I\neq 0$ are oriented in relation to their quantization axis, which in most cases is taken to be the direction of the bombarding-particle beam. The degree of orientation of the nuclei depends on the reaction mechanism and on the process of de-excitation of the initial excited state.

Nuclear orientation can be described in terms of the filling parameter $P(m)$, which determines the probabilities of population of the sublevels with quantum numbers m. It is convenient to distinguish two forms of nuclear orientation: polarization and alignment (Fig. 2). In polarization of a state with spin $I>0$ the parameter has the property $P(m)\neq P(-m)$. Polarization of nuclei is observed, for example, in measurements of the asymmetry of β decay. In alignment of states with spin $I>1/2$ the parameter has the property $P(m)=P(-m)$, but for different absolute values $|m|$ the value of $P(m)$ is different. Alignment can be observed in measurements of the anisotropy of γ radiation, which is determined by the formula

$$W(\theta)=1+A_2P_2(\cos\theta)+A_4P_4(\cos\theta)+\ldots, \quad (1)$$

where P_{2k} are Legendre polynomials.

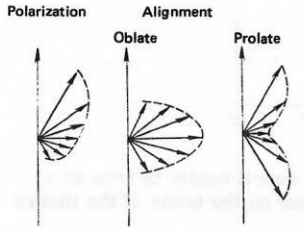

FIG. 2. Polarization and alignment of nuclei.

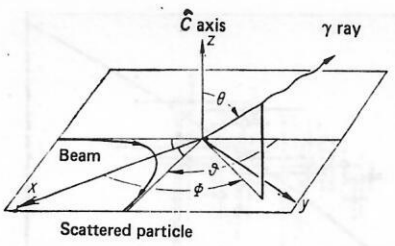

FIG. 3. Scattering geometry in Coulomb excitation: $\hat{C}$ is the crystalline symmetry axis.

The nuclear orientation in Coulomb excitation can be found theoretically.[1] The scattering geometry is shown in Fig. 3, and the dependence of the probability for formation of polarized nuclei in the excitation $0^+\rightarrow 2^+$ on the scattering angle of the exciting particle is shown in Fig. 4.

In fusion reactions a large angular momentum of the system of colliding nuclei leads to the creation of strongly aligned compound nuclei. In the fusion of two nuclei with spins equal to zero, the compound nucleus will be completely aligned since $P(0)=1$, while for $m\neq 0$ we have all $P(m)=0$. In fusion of nuclei with spins I_T (the target nucleus) and I_B (the bombarding nucleus) the initial state of the compound nucleus also will be strongly aligned with a population distribution between the two extreme values $m=\pm(I_T+I_B)$ (oblate alignment).

On emission of neutrons from the initial state of the compound nucleus, the distribution of the sublevel populations is broadened; the contribution of neutron emission to the width of this distribution can be estimated by means of the approximation of one-dimensional disordered motion. If the emission of one neutron changes m by Δm, then emission of x neutrons gives a contribution to the distribution width

$$\sigma_n(m)=\Delta m\sqrt{x}. \quad (2)$$

After neutron emission a lower isomeric state, which is interesting from the point of view of the study of hyperfine interactions, is reached with emission of a cascade of γ rays. Gamma transitions can also decrease the alignment of a nuclear-reaction product, but to an insignificant degree, since a preference exists for cascade γ rays of the prolate type, which carry away angular momentum but do not affect the nuclear alignment.

The preservation of a significant alignment of the ground-state rotational band was proved experimentally

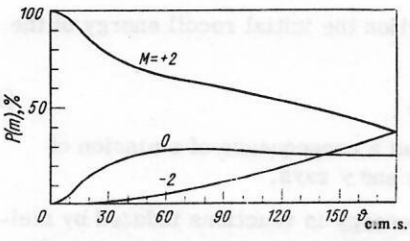

FIG. 4. Probability of population of various sublevels m in Coulomb excitation $0^+\rightarrow 2^+$ with use of the scattering geometry shown in Fig. 3 [$P(\pm 1)=0$]: $\xi=0.2$ is the adiabaticity parameter.

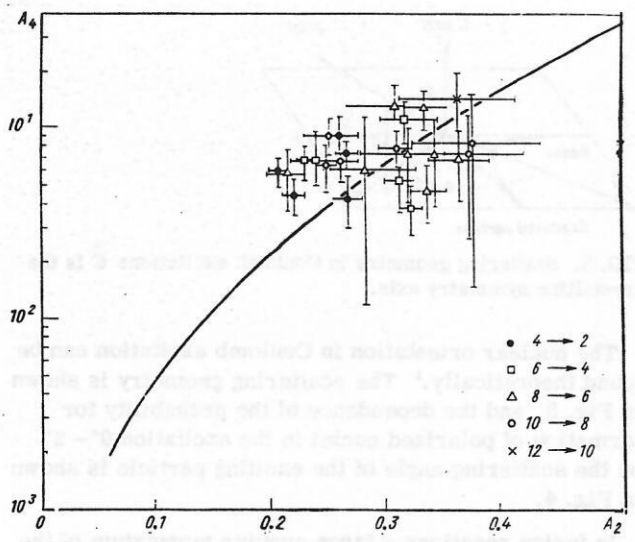

FIG. 5. Relation of the coefficients A_2 and A_4 of the γ-ray angular distribution for a number of rotational and vibrational transitions which are the last steps of γ cascades from high-spin states populated in reactions induced by multiply charged ions. The coefficients for the transitions $2 \rightarrow 0$ have not been included, since they can be suppressed as the result of hyperfine interactions.[3]

by Diamond *et al.*[2] and by Newton *et al.*[3] in measurements of the angular distribution of type $E2\gamma$ rays. Measured values of the angular distribution coefficients A_2 and A_4 are shown in Fig. 5. They agree with values predicted for oblate alignment with a width of the Gaussian distribution of the sublevel populations $\sigma(m)$ close to two.

We can attempt a more rigorous approach to the theoretical determination of the change of alignment in transitions from the initial state of the compound nucleus (see, for example, Ref. 4), but for applications of methods of studying hyperfine interactions in accelerator beams the existence of nuclear orientation, which is confirmed in many experiments, is significant.

Recoil of nuclear products. In Coulomb excitation the maximum recoil energy (in backward scattering of the exciting particle) is

$$T=\frac{M_1M_2T_i}{(M_1+M_2)^2}\left(1+\sqrt{1-\frac{\Delta E}{T_i}\left(1+\frac{M_1}{M_2}\right)}\right)^2, \quad (3)$$

where M_1 and M_2 are the masses of the bombarding particle and the target nucleus, T_i is the energy of the incident ion, and ΔE is the excitation energy of the target nucleus.

For a fusion reaction the initial recoil energy of the compound nucleus

$$T=T_iM_1/(M_1+M_2) \quad (4)$$

changes somewhat as a consequence of emission of secondary particles and γ rays.

The large recoil energy in reactions induced by multiply charged ions permits implantation of the reaction products in various materials (ferromagnets, single crystals with a definite direction of the axis of the electric field gradient, and so forth) for creating appropriate conditions for the study of hyperfine interactions.

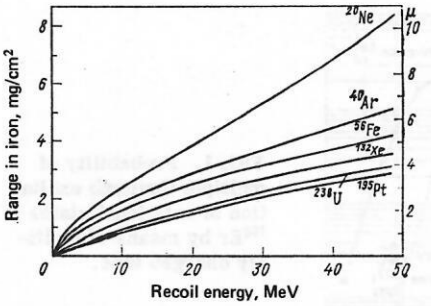

FIG. 6. Range of reocil nuclei in iron as a function of their energy.

Tables of the ranges and stopping powers of nuclei of various energies in various materials have been composed by Northcliffe and Schilling[5] on the basis of the theory of Lindhard *et al.*[6] For illustration we have shown in Fig. 6 the range of a number of nuclei in iron as a function of their energy. The slowing-down time can also be calculated on the basis of Lindhard's theory. In Fig. 7 we have shown the slowing-down time in iron as a function of energy. It is evident from this figure that even at high recoil energies the slowing-down time does not exceed 1.5 psec.

2. INTERACTION OF NUCLEAR MOMENTS WITH EXTRANUCLEAR FIELDS

All experimental methods of studying hyperfine interactions of nuclear moments (magnetic dipole and electric quadrupole moments) with extranuclear fields (magnetic field and electric field gradient) reduce to direct measurement of the interaction energy, i.e., the energy splitting of nuclear levels, or to measurement of the frequencies of rotation of the nuclear spin around the magnetic field direction or around the electric field gradient axis. For a magnetic dipole interaction, only one frequency, the Larmor precession frequency, is observed, which is identical for all sublevels of a given nuclear state. For an electric quadrupole interaction the precession frequency depends on the quantum number m, and the direction of precession changes sign in the transition from $+m$ to $-m$. Therefore the method of the perturbed angular distribution (PAD) of γ rays permits observation of rotation of an aligned nucleus

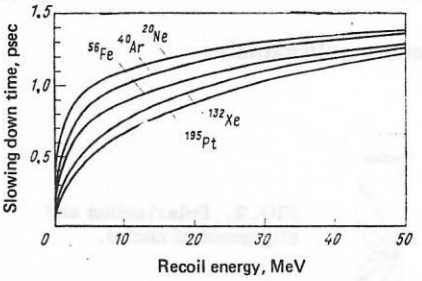

FIG. 7. Time of slowing down of recoil nuclei in iron as a function of their energy, calculated on the basis of the theory of Lindhard *et al.*[6]

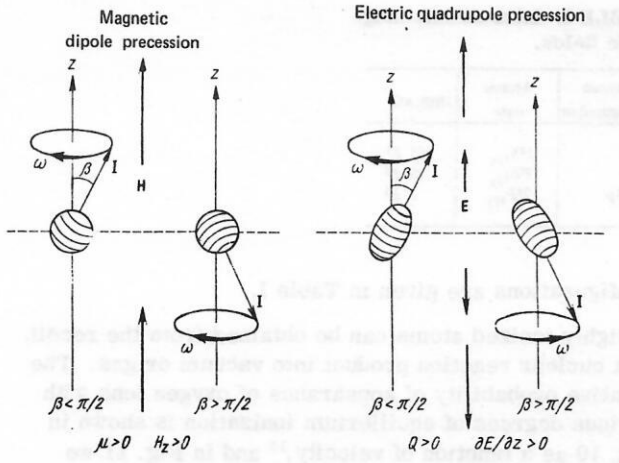

FIG. 8. Difference between classical magnetic dipole and electric quadrupole precession.

only for a magnetic interaction. The electric quadrupole interaction of aligned nuclei does not lead to rotation of the γ-ray angular distribution pattern, since the rotations for the states $+m$ and $-m$ cancel each other. Rotation of the γ-ray angular distribution can be observed only for polarized nuclei interacting with an electric field gradient oriented in a single crystal.

The difference between the classical Larmor precession and the quadrupole precession is shown in Fig. 8.

Magnetic dipole interaction. The interaction energy of a nuclear magnetic moment

$$\mu = gI\mu_N \tag{5}$$

(the nuclear magneton is $\mu_N = 3.152 \times 10^{-12}$ eV/G) with a magnetic field **H** is expressed by the formula

$$E_m = -\boldsymbol{\mu}\cdot\mathbf{H} = -\mu H_m/I = -mg\mu_N H, \tag{6}$$

and the energy splitting of the sublevels

$$\Delta E_m = \mu H/I = g\mu_N H \tag{7}$$

can be written in the form

$$\Delta E_m = \omega_M \hbar,$$

where the Larmor precession frequency is

$$\omega_M = -g\mu_N H/\hbar = -4.790\times10^3 gH \text{ (G)}, \text{ rad/sec}.$$

The integral method of perturbed angular distributions (IPAD) measures the average rotation angle of the γ-ray distribution pattern during the lifetime τ of the excited state of a nucleus subjected to a magnetic interaction:

$$\theta = \omega_M \tau. \tag{8}$$

In very favorable cases with $g = 0.5$ a rotation angle of 1 mrad can be measured with an accuracy down to 20%. It follows from this that to carry out measurements with this accuracy for a nuclear state with lifetime $\tau = 1$ nsec a magnetic field $H = 0.4$ MG is necessary. Such fields cannot be produced even with superconducting magnets. However, fields of substantially greater intensity exist in nature—the fields acting on nuclei in magnetic materials and in highly ionized atoms.

Sources of ultrahigh magnetic fields. (*I*) *Internal magnetic fields in magnetic materials.* Large internal fields in magnetic materials were first observed (independently at Moscow and at Oxford) by the method of nuclear orientation at low temperatures. B. N. Samoĭlov *et al.*[7] showed that a magnetic field of about 1300 kG acts on Au nuclei in iron, and Grace *et al.*[8] observed a field close to 200 RG affecting the Co nucleus in metallic Co. At the present time the magnetic fields acting in Fe on the nuclei of most elements have been determined. We also know the values of the internal magnetic fields which act on various nuclei in the lattices of Ni, Co, and Gd and other rare earth elements, and also in lattices of a number of alloys and chemical compounds which have magnetic properties.

The internal magnetic field H_{int} is made up of the local field and the hyperfine-structure field:

$$\mathbf{H}_{int} = \mathbf{H}_{loc} + \mathbf{H}_{hf}. \tag{9}$$

The local field is determined by the external magnetic field H_{ext}, the magnetizing field, and the Lorentz field:

$$\mathbf{H}_{loc} = \mathbf{H}_{ext} + 4\pi\mathbf{M}'/3 - D\mathbf{M}, \tag{10}$$

where **M** is the magnetization, **M′** is the domain magnetization (**M′** = **M** in paramagnetic materials), and D is the demagnetization factor. The local field is not large, of the order of tens of kilogausses.

The hyperfine-structure field is made up of the following contributions:

1) The field produced by the orbital motion of the electrons. For transition elements of the Fe group it is of the order of 10^4 G if the orbital angular momentum is not completely frozen, and for rare earth elements this field is dominant and amounts to about 10^6–10^7 G;

2) the dipole field, which is produced by the spin magnetic moments of the electrons surrounding the ions. It is of the order of 10^4 G and disappears for cubic symmetry of the crystal lattice;

3) the Fermi contact field produced by the difference in density of electrons with opposite spin directions; it is of the order of 10^5 G.

There are several theories which predict values of the hyperfine fields acting in magnetic materials on nuclei of various elements, but none of them as yet permit accurate determination of the fields. Using these fields, it is possible to carry out measurements in the picosecond lifetime region of nuclear states. Polarization of the internal fields can be accomplished by means of an external magnetizing field. For saturation of a ferromagnetic foil usually several hundred gausses is sufficient.

(*II*) *Transient magnetic fields* of large value acting in a magnetized ferromagnetic material on a moving nucleus were observed in 1967 by Grodzins.[9] The theory developed by Lindhard and Winther[10] explains the appearance of transient fields as the result of the scattering of polarized electrons of a ferromagnetic material on the moving nucleus. This scattering increases the density of polarized electrons in the nuclear volume and creates a magnetic field through the Fermi contact interaction. According to the theory of Lindhard and

Winther, the transient field should be proportional to the atomic number Z of the moving nucleus and its dependence on the velocity of the nucleus should have the following form:

$$H(v) \sim 1/v \text{ for } v > v_p, \quad (11)$$

where $H(v)$ does not depend on velocity for $0 < v \leq v_p$, where v_p is the velocity of the polarized electrons in the given ferromagnetic material.

Recently it has been observed[11-14] that the transient fields are significantly higher than predicted by Lindhard and Winther. In 1976 Eberhardt *et al.*[15] showed that the transient magnetic field acting in Fe on a ^{28}Si recoil nucleus increases linearly with velocity. These authors gave a phenomenological formula describing the dependence of the transient field on the value of Z of the moving nucleus and on its velocity v:

$$H = aRZ(v/v_p)^p, \quad (12)$$

where R is a relativistic coefficient[10] which plays a role for $Z \geq 30$. Empirical values of the parameters a and p were obtained from experiments with ^{28}Si:

$$a = (125 \pm 17)\,\text{kG}, \quad p = 10.5 \pm 0.25.$$

The angle of precession of ^{28}Si in the transient field of Fe is shown in Fig. 9 as a function of velocity. The disagreement with the predictions of the theory of Lindhard and Winther is quite evident. The authors[15] explain this result by assuming that the main process responsible for appearance of the transient fields is the capture of polarized electrons of the ferromagnetic material in $1s$ and $2s$ holes in the electron shell of the moving ion.

(III) Magnetic fields in free highly ionized atoms. In free atoms containing only a few electrons in internal shells the magnetic fields acting on the nucleus may have rather large values. An unpaired electron with quantum numbers n, l, j produces at the nucleus a magnetic field

$$H(0)_j = \frac{hc\alpha^2 R_\infty}{\mu_B} \frac{Z^3}{n^3 (l+1/2)(j+1)}, \quad (13)$$

where μ_B is the Bohr magneton, α is the fine structure constant, and R_∞ is the Rydberg constant. The intra-atomic magnetic fields for several simple electron configurations are given in Table I.

TABLE I. Intra-atomic magnetic fields.

Electronic configuration	Atomic state	$H(0)$, kG
$1s$	$1^2S_{1/2}$	$167\,Z^3$
$1s^22s$	$2^2S_{1/2}$	$15\,Z^3$
$1s^22s^2p$	$2^2P_{1/2}$	$3\,Z^3$

Highly ionized atoms can be obtained from the recoil of a nuclear reaction product into vacuum or gas. The relative probability of appearance of oxygen ions with various degrees of equilibrium ionization is shown in Fig. 10 as a function of velocity,[16] and in Fig. 11 we have given a universal curve of equilibrium charge as a function of reduced velocity.[17]

Electric quadrupole interaction. The interaction energy of a nuclear quadrupole moment Q with an electric field gradient of axial symmetry eq is expressed as follows:

$$E_Q(m) = e^2Qq\,[3m^2 - I(I+1)]/[4I(2I-1)]. \quad (14)$$

The energy splitting of the sublevels with quantum numbers m and $m-1$,

$$\Delta E_Q = e^2Qq\,3(2m-1)/[4I(2I-1)], \quad (15)$$

can be expressed in terms of the quadrupole precession frequency ω_Q as

$$\Delta E_Q = \omega_Q \hbar, \quad (16)$$

where

$$\omega_Q = \frac{e^2Qq}{\hbar} \frac{3(2m-1)}{4I(2I-1)}. \quad (17)$$

This expression can be written in the form

$$\omega_Q = 3(2m-1)\,\omega_E; \quad (18)$$

here

$$\omega_E = \frac{e^2Qq}{4I(2I-1)\hbar} = 3.8 \cdot 10^{14} \frac{eq\,(\text{V/cm}^2)\,Q\,(\text{cm}^2)}{I(2I-1)}\ \text{rad/sec} \quad (19)$$

is the fundamental quadrupole frequency. For integral values of I the quadrupole precession frequencies are $\omega_Q = 3\omega_E$, $9\omega_E$, $15\omega_E \ldots$, and for half-integral I we have $\omega_Q = 6\omega_E$, $12\omega_E$, $18\omega_E, \ldots$. If the electric field gradient does not have axial symmetry, then the gradient tensor is determined by two parameters: the z component V_{zz}, which is usually designated eq, and the

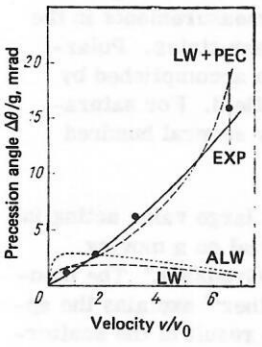

FIG. 9. Variation of the precession angles of the ^{28}Si excited state in a transient field in iron according to the predictions of Lindhard and Winther (LW) ($v_p = 0.78v_0$) and according to the modified theory of the same authors (ALW) ($v_p = 0.43v_0$). Satisfactory agreement is obtained when polarized-electron capture is taken into account (LW+ PEC).[15]

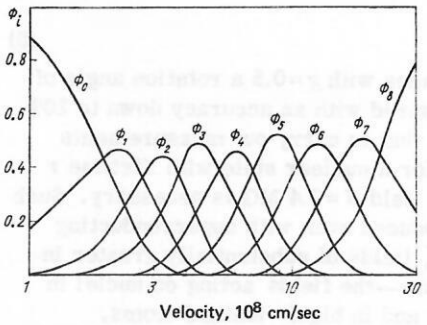

FIG. 10. Relative probability of equilibrium ionization of oxygen atoms as a function of their velocity: Φ is the fraction of i-fold ionized atoms in the beam.[16]

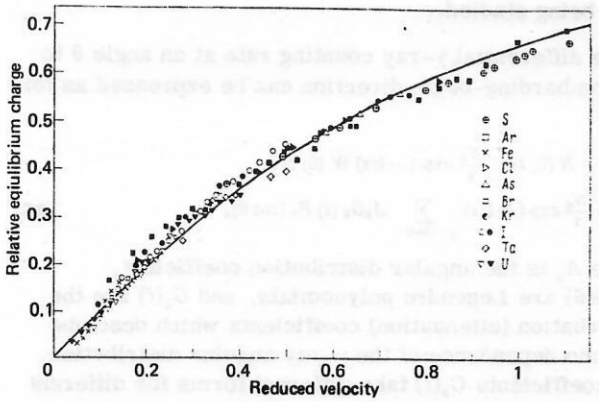

FIG. 11. Average equilibrium charge of ions after stripping in a foil, as a function of the reduced velocity $v/(v'Z^{0.45})$ ($v' = 3.8 \times 10^8$ cm/sec).[17]

asymmetry parameter

$$\eta = |V_{xx} - V_{yy}|/V_{zz}. \quad (20)$$

The x, y, and z axes are chosen so that the condition $|V_{xx}| \leq |V_{yy}| \leq |V_{zz}|$ is satisfied; in this case the values of the parameter η are in the range $0 \leq \eta \leq 1$. The interaction Hamiltonian is

$$\mathcal{H}_Q = \frac{e^2Qq}{4I(2I-1)}\left[3I_z^2 - I(I+1) + \frac{\eta}{2}(I_+^2 + I_-^2)\right]. \quad (21)$$

When η is not equal to zero, m is not a good quantum number and the split sublevels do not have definite values of m. For integral spins the degeneracy in the sign of the projection of the angular momentum, which existed for a field gradient of axial symmetry, is completely lifted, while for half-integral spins the degeneracy remains. Thus, for $I = 1$

$$E_0 = -e^2qQ/2; \quad E_1 = e^2qQ(1 \pm \eta)/4; \quad (22)$$

for $I = 3/2$

$$E_{1/2} = -e^2qQ(1 + \eta^2/3)^{1/2}/4; \quad E_{3/2} = e^2qQ(1 + \eta^2/3)^{1/2}/4. \quad (23)$$

In contrast to the static magnetic dipole interaction, the static electric quadrupole interaction does not give for aligned nuclei a resultant precession, and therefore there is also no rotation of the γ-ray angular distribution. With the perturbed angular distribution method a periodic variation of the γ-ray anisotropy is observed which is due to superposition of a series of quadrupole frequencies. Since the periodic weakening of the angular distribution is an even function of the frequency ω_E, experiments with aligned nuclei do not permit determination of the sign of the quadrupole interaction. Nuclear precession appears only in experiments with polarized nuclei interacting with an oriented electric field gradient, and only in such experiments is it possible to determine the sign of the interaction.[18]

Under laboratory conditions it is impossible to produce a sufficiently strong electric field gradient for observation of the hyperfine quadrupole interaction. Such gradients exist in noncubic crystal lattices. In metals the electric field gradient is due to two factors: the distribution of charges in the crystal lattice sites and the distribution of conduction electrons. Both contributions q^{latt} and q^{el} create in the nucleus an electric field gradient modified by the deformation of the electron shells of the given atom:

$$q = (1 - \gamma_\infty) q^{\text{latt}} + (1 - R_Q) q^{\text{el}}, \quad (24)$$

where γ_∞ and R_Q are the antiscreening coefficients. The electric field gradients acting on nuclei in crystals reach 10^{19} V/cm^2.

Nuclear spin relaxation. It is necessary to distinguish static hyperfine interactions and hyperfine interactions which depend on time. Static interactions do not destroy the nuclear alignment and give only a periodic variation of the γ-ray angular distribution. Interactions which depend on time lead to a damping of the nuclear alignment and as a consequence of this to an irreversible decrease of the γ-ray anisotropy. This damping is described by the nuclear spin relaxation time T_r, which is related to the correlation time τ_c by the following expression, which depends on the nature of the fluctuation of the direction or magnitude of the magnetic field acting on the nucleus:

$$T_r \approx 1/(\omega^2\tau_c), \quad (25)$$

where ω is the average frequency of nuclear precession in a given fluctuating field.

The theory of weakening of the γ-ray angular isotropy produced by a time-dependent perturbation satisfying the condition $\tau_c\omega \ll 1$ was originated by Abragam and Pound.[19] A more general theory has been given by Blume.[20]

It is possible to enumerate many causes of spin relaxation. In solids it is due to fluctuations of the direction of the electron spin of paramagnetic atoms or to the influence of lattice defects. Relaxation in liquids is produced by translation and rotational motions of the molecules, and for highly ionized atoms moving in a gas it will be produced by atomic collisions and optical transitions.

If experiments are carried out with long-lived nuclear states and their purpose is not to study the spin-relaxation process as such, then it is necessary to introduce the nuclear reaction products being studied into a medium in which relaxation will occur as slowly as possible. For this purpose one can recommend diamagnetic cubic crystals without impurities or radiation damage, and also molten metals. Gases are also a good medium if the atoms which are being slowed down are in a spinless state. In some cases (for example, for recoil into a vacuum) the use of a sufficiently high longitudinal magnetic field (in the direction of the symmetry axis of the system) will permit the orientation of the nuclei to be retained and will lead to an unweakened angular distribution. The degree of destruction of the coupling for recoil in a vacuum is determined by the ratio $\mu_N g H(0) I/\mu_B g_J H_z J$, from which it follows that the magnetic field H_z necessary for almost complete destruction of the coupling should be of the order

$$H_z \approx 10\,(\mu_N g I/\mu_B g_J J)\, H(0).$$

3. METHODS OF STUDY OF HYPERFINE INTERACTIONS IN CHARGED-PARTICLE BEAMS

Most methods of studying hyperfine interactions in charged-particle beams are based on observation of the

perturbation of the angular distribution of the γ rays emitted by excited nuclei aligned as the result of a nuclear reaction and which during their lifetime are subjected to the action of extranuclear electromagnetic fields. The perturbed angular distribution of γ rays can be treated by application of the theory of perturbed angular γ correlations[21] (PAC), taking as the quantization axis the direction of the beam of bombarding particles instead of the direction of emission of the first of the photons of the γ cascade. In the PAD method the restriction to a long lifetime of the excited nuclear state, which in the PAC method is due to coincidence counting, is removed. (In the PAC method for a lifetime of the order of 1 μsec the large ratio of the number of accidental coincidences to the number of true coincidences limits the possibility of measurement.) Since in the PAD method γ-ray singles spectra are recorded, this restriction no longer exists.

Other methods are based on combination of the method of the angular distribution of the nuclear radiation with nuclear magnetic resonance (NMR-PAD). A field with a frequency corresponding to the splitting of the nuclear sublevels, producing transitions between them, equalizes their population, the orientation of the nuclei disappears, and the nuclear radiation from a given excited state becomes isotropic.

A third method which can be applied to the study of hyperfine interactions in-beam is Mössbauer spectroscopy. However, up to the present time Mössbauer spectroscopy in-beam has not yet found extensive application and the number of studies carried out by this method is small.

A comparison of the various methods of studying hyperfine interactions in-beam as a function of the lifetime of the excited states is given in Fig. 12. The limitations of the various methods are also indicated in the figure.

Differential method of perturbed γ-ray angular distributions (DPAD). The differential method of perturbed angular correlations, which was used for the first time[22] in 1959, can be used to study hyperfine interactions in-beam without substantial changes. The time which is equal to zero is specified in this case not by the first γ ray of the cascade, but by the beam pulse at the target or by the particle emitted in the nuclear reaction which leads to excitation of the excited nuclear state being studied.

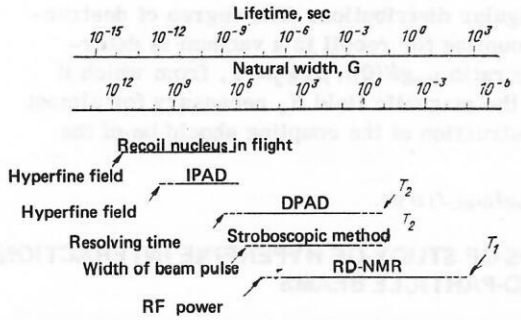

FIG. 12. Comparison of different methods of study of hyperfine interactions in-beam (from Ref. 4).

The differential γ-ray counting rate at an angle θ to the bombarding-beam direction can be expressed as follows:

$$N(\theta, t) = \frac{N_0}{\tau} \exp(-t/\tau)\, W(\theta, t)$$
$$= \frac{N_0}{\tau} \exp(-t/\tau) \sum_{k \text{ even}} A_k G_k(t) P_k(\cos\theta), \quad (26)$$

where A_k is the angular distribution coefficient, $P_k(\cos\theta)$ are Legendre polynomials, and $G_k(t)$ are the perturbation (attenuation) coefficients which describe the time dependence of the γ-ray angular distribution. The coefficients $G_k(t)$ take different forms for different forms of hyperfine interaction perturbing the angular distribution. We shall give several examples.

1. Static magnetic interaction

a) For a polycrystalline unmagnetized ferromagnetic material

$$G_k(t) = (2k+1)^{-1} \sum_{-k}^{+k} \cos(k\omega t), \quad (27)$$

where ω is the Larmor precession frequency of the magnetic field acting on the nuclei studied;

b) for a magnetic field perpendicular to the plane formed by the axis of the bombarding beam and the γ-ray detector.

The perturbed angular distribution function is conveniently written in the form

$$W(\theta, \pm H, t) = 1 + \sum_k b_k \cos k(\theta \mp \omega t). \quad (28)$$

The coefficients b_k are expressed in terms of the A_k as follows:

$$b_2 = \frac{3A_2/4 + 5A_4/16}{1 + A_2/4 + 9A_4/64}; \quad b_4 = \frac{35A_4/64}{1 + A_2/4 + 9A_4/64}. \quad (29)$$

Usually measurements of the counting rate $N(\theta, t)$ are made for an angle $\theta = 45°$ and for two opposite directions of the magnetic field $\pm H$, after which the following ratio is calculated:

$$R(t) = \frac{N(45°, +H, t) - N(45°, -H, t)}{N(45°, +H, t) + N(45°, +H, t)} = \frac{b_2 \sin 2\omega t}{1 + b_4 \cos 4\omega t}, \quad (30)$$

which no longer depends on the lifetime τ. If b_4 can be neglected, then $R(t)$ has the form of a sinusoidal curve with a period equal to half the period of the Larmor precession.

In measurements in an external magnetic field it is necessary to take into account a correction to the angle θ due to the deflection of the bombarding beam. In a uniform magnetic field H the deflection of a beam of particles with mass number A, charge z, and velocity v traveling a distance l is

$$\Delta\theta = 3.22 \cdot 10^{-7} \frac{lzH\,(\mathrm{G})}{Av/c} \text{ rad}. \quad (31)$$

As an example we show in Fig. 13 the curve $R(t)$ for a magnetic field of 117 G for the 3.46-MeV 7^+ 22-μsec state of ^{38}K obtained in the reaction ^{35}Cl(α, n) in the pulsed beam of the Bucharest cyclotron.[23]

2. Static electric quadrupole interaction

For an axially symmetric electric field gradient

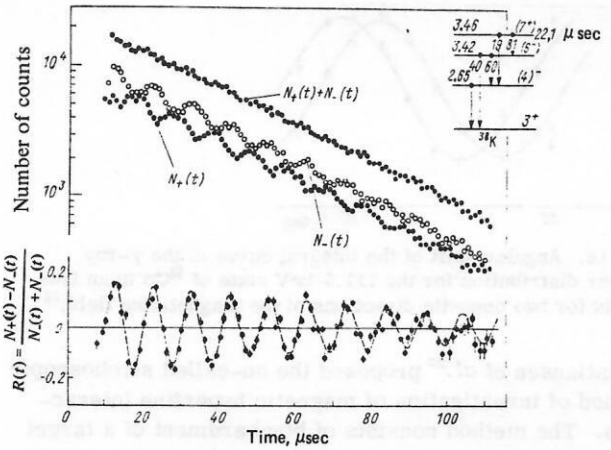

FIG. 13. Larmor precession $R(t)$ in an external magnetic field for the 22-μsec state of ^{38}K (Ref. 23).

randomly distributed in a polycrystalline material:

$$G_k(t)=\sum_n s_{kn}\cos(n\omega_E t), \tag{32}$$

where

$$s_{kn}=\sum_{m,m'}\begin{pmatrix} I & I & k \\ m' & -m' & -m'+m \end{pmatrix} \tag{33}$$

and ω_E is the fundamental quadrupole frequency. The summation over m and m' is carried out for those values which give the corresponding quadrupole frequencies ω_Q. The differential method is used to measure the periodic attenuation curve

$$R(t)=(2\cdot3)\,(W(0^\circ,t)/W(90^\circ,t)-1), \tag{34}$$

which for $A_4=0$ has the form

$$R(t)=A_2G_2(t). \tag{35}$$

An example of quadrupole perturbation is shown in Fig. 14. Here we show curves $R(t)$ obtained by Haas *et al.*[24] for the 398-keV $9/2^+$ 4-msec state of ^{69}Ge in Zn and Ga, obtained in the reactions ^{66}Zn(α,n) and ^{69}Ga(p,n). Since the spin of the excited state of ^{69}Ga is 9/2, the curves shown in the figure are the result of a superposition of four quadrupole frequencies.

In experiments with a pulsed beam the differential method can be used if we satisfy the conditions

$$\Delta T\ll\pi/\omega\leqslant T,\quad T\geqslant\tau, \tag{36}$$

where ΔT is the width of the beam pulse and T is the distance between pulses. The width of the beam pulse limits the application of the differential method for excited states with lifetimes greater than several nanoseconds. If the measurement is made in coincidence with a particle emitted in a nuclear reaction, the limiting factor is the time resolution of the fast coincidence circuit. In this case, differential measurements can be carried out with somewhat shorter-lived states.

Measurements for states with much shorter lifetimes can be carried out with a new version of the differential method based on the time-of-flight principle. The nuclei of highly ionized atoms emitted from a target into vacuum have acting on them huge magnetic fields produced by the unpaired electrons. The time dependence of the angular distribution of the emitted γ rays can be followed by varying the distance between the target and the stopper in which the ions are retained. At the moment of stopping of an ion in a stopper with a cubic crystal lattice, the perturbation ceases to act and the angle of rotation of the γ-ray distribution is frozen. By measuring the ratio $R(t)$ of the γ-ray intensities for angles of 90° and 135° (or 45°) with respect to the beam direction, one obtains an oscillating function which is used for calculation of the Larmor frequency ω.

For a hydrogen-like ion with one electron in the ground state the time dependence of the perturbation of the γ-ray angular distribution is described by the coefficient

$$G_k(t)=1-G(\omega,t)\,k(k+1)/(2I+1)^2, \tag{37}$$

where

$$G(\omega,t)=1-\exp(-t/\tau)\cos\omega t$$
$$-[1+\exp(-t/\tau)\,(\omega\tau\sin\omega t-\cos\omega t)]/[1+(\omega\tau)^2]; \tag{38}$$

here ω is the Larmor frequency in the intra-atomic magnetic field and $t=d/v$ is the time of flight of a nu-

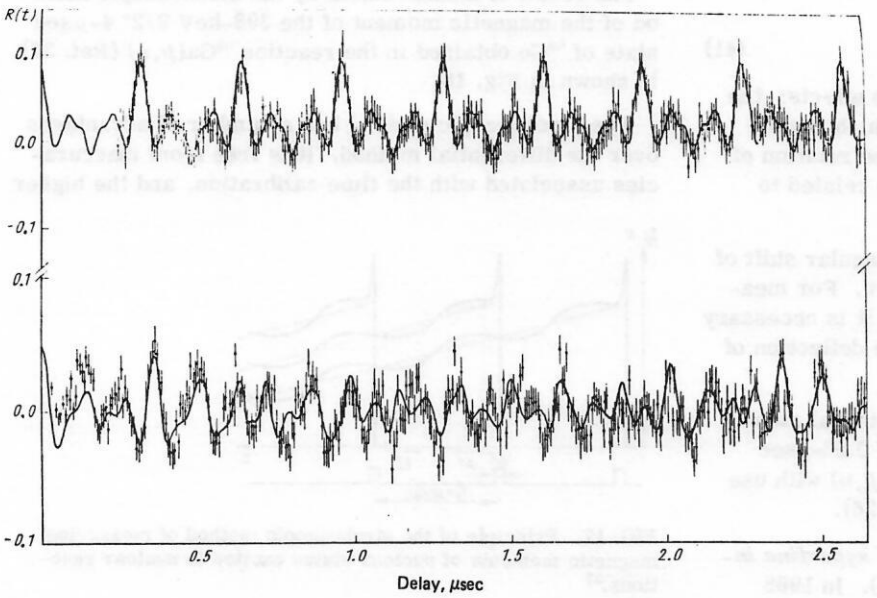

FIG. 14. Quadrupole interaction of the 4-msec state of ^{69}Ge in Zn (300°C) and Ga (–20°C) (Ref. 24). The experimental values of $R(t)$ are compared with $A_2G_2(t)$ with inclusion of an asymmetry parameter $\eta=0.697$ for the Ga matrix.

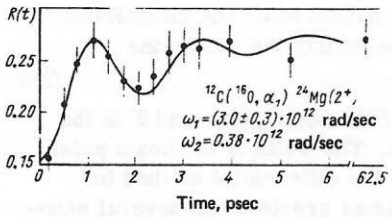

FIG. 15. The ratio $R(t)$ for the 1.75-nsec state of ^{24}Mg moving in vacuum.[25]

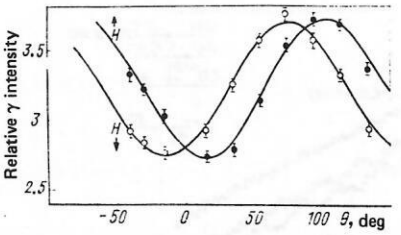

FIG. 16. Angular shift of the integral curve of the γ-ray angular distribution for the 111.5-keV state of ^{58}Co in an iron matrix for two opposite directions of the magnetizing field.[26]

cleus with velocity v over a distance d between the target and the stopper.

The interpretation of the measurements is simplified if the use of a Ge(Li) γ detector with good energy resolution permits distinguishing the Doppler-shifted γ line which corresponds to emission of γ rays by moving nuclei and the unshifted line corresponding to stopped nuclei. In this case the coefficients $G_k(t)$ for the unshifted γ line have the simpler form:

$$G_k(t)=1-(1-\cos\omega t)\,k(k+1)/[(2I+1)^2]. \tag{39}$$

The result of measurement of the interaction with an intra-atomic magnetic field of the 1.37-MeV 2^+ 1.75-nsec state of ^{24}Mg, obtained in the ^{16}O beam of the Utrecht accelerator in the reaction $^{12}C(^{16}O, \alpha)$ (Ref. 25), is shown in Fig. 15. From the $R(t)$ curve the authors find two Larmor frequencies, the higher of which they assign to the 1s state of the Mg atoms.

Integral measurement of perturbed angular distributions of γ rays (IPAD). For a short lifetime of the excited state of the nucleus, when measurements by the differential method are impossible, one can measure the integral effect of γ-ray angular distribution perturbation. The integral function of the angular distribution perturbed by a transverse magnetic field has the form

$$\overline{W(\theta,\pm H)}=\frac{1}{\tau}\int_0^\infty \exp(-t/\tau)\,W(\theta,\pm H,t)\,dt$$
$$=1+\sum_{k\ (\text{even})}\frac{b_k}{\sqrt{1+(k\omega\tau)^2}}\cos k(\theta\mp\Delta\theta_k), \tag{40}$$

where

$$\Delta\theta_k=(1/k)\operatorname{arctg}k\omega\tau. \tag{41}$$

In Eq. (40) we have taken into account two effects: the attenuation of the angular distribution, which is described by a factor $[1+(k\omega\tau)^2]^{-1/2}$, and the rotation of the angular distribution pattern, which is related to $\Delta\theta_k$.

If b_4 can be neglected and $\omega\tau \ll 1$, the angular shift of the γ-ray distribution curve is equal to $\omega\tau$. For measurement with an external magnetic field it is necessary to remember the correction $\Delta\theta$ due to the deflection of the beam.

In Fig. 16 we show an example of the integral measurement of the g factor of the 111.5-keV 0.26-nsec state of ^{58}Co excited in the reaction $^{85}Fe(p,n)$ with use of the internal magnetic field in Fe (Ref. 26).

Stroboscopic method of investigation of hyperfine interactions in an accelerator beam (SIPAD). In 1968 Christiansen *et al.*[27] proposed the so-called stroboscopic method of investigation of magnetic hyperfine interactions. The method consists of bombardment of a target by a pulsed beam of accelerated particles with a repetition frequency f which corresponds to a harmonic of the Larmor precession frequency of excited nuclei obtained in a nuclear reaction:

$$f=1/T=\omega/\pi n,\ n=1,\ 2,\ 3,\ \ldots, \tag{42}$$

where T is the time interval between beam pulses. The principle of the stroboscopic method is illustrated in Fig. 17. The γ rays of aligned nuclei formed during the pulse have a definite angular distribution, rotation of which in a magnetic field modulates the decay curve of the excited state. If condition (42) is satisfied, the modulation of the decay curves which accompany the recurring pulses coincides in phase with the decay itself, and the effect of the Larmor precession is enhanced. This can be observed by means of two counters located at angles $+45°$ and $-45°$ to the bombarding-beam direction and recording after each pulse the number of counts in the time intervals (windows) designated in Fig. 17 by the letters A_1 and A_2. If one counter ($+45°$) records in these time intervals the numbers of counts N_1^+ and N_2^+, and the other ($-45°$) records N_1^- and N_2^-, then the ratio $N_1^+N_2^-/N_1^-N_2^+$ is a sensitive measure of the degree of agreement of the beam-pulse repetition frequency with the Larmor frequency. Measurement of the ratio as a function of the magnetic field strength gives a sharp minimum when these frequencies correspond.

The result of measurement by the stroboscopic method of the magnetic moment of the 398-keV $9/2^+$ 4-μsec state of ^{69}Ge obtained in the reaction $^{69}Ga(p,n)$ (Ref. 27) is shown in Fig. 18.

The stroboscopic method has a number of advantages over the differential method. It is free from inaccuracies associated with the time calibration, and the higher

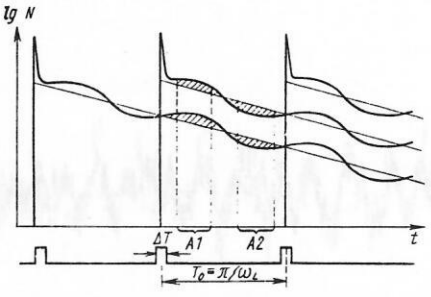

FIG. 17. Principle of the stroboscopic method of measuring magnetic moments of nuclear states excited in nuclear reactions.[27]

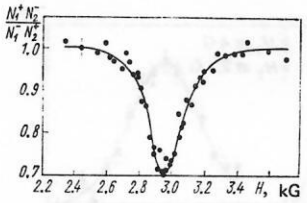

FIG. 18. Resonance curve for the 398-keV state of ^{69}Ge, obtained by the stroboscopic method.[27]

frequency of the impulses permits operation with higher average currents of accelerated particles, which reduces the measurement time.

Application of the stroboscopic method to study of the electric quadrupole interaction has been discussed by Bosse and Gabriel.[28] The performance of the experiment is complicated by the fact that for a fixed value of the electric field gradient in a crystal it is necessary to change the frequency of the beam pulses. This was done by Schatz *et al.*,[29] who were able to obtain a stroboscopic quadrupole resonance for ^{69}Ge in metallic Zn (Fig. 19).

Radiofrequency detection of nuclear magnetic resonance (RD-NMR). The essence of methods based on radiofrequency detection of nuclear magnetic resonance consists of radiofrequency irradiation of oriented nuclei in which the magnetic sublevels of an excited state are populated nonuniformly, and in observation of NMR by measurement of the intensity of nuclear radiation as a function of the radio frequency or magnetic field strength. These methods combine a high accuracy in determination of the resonance frequency with the high sensitivity of methods of detecting nuclear radiation. Their accuracy depends on the width of the resonance line, which is determined either by the lifetime of the nuclear state being studied or by the nuclear spin relaxation time.

The RD-NMR method was first used in 1952 by Deutsch and Brown[30] in measurements of the hyperfine structure of positronium. In 1959 Connor[31] used it to determine the magnetic moment of the ground state of ^{8}Li (0.84 sec) obtained by capture of polarized neutrons in ^{7}Li.

The development of various forms of the RD-NMR method has been stimulated by the discovery of the hyperfine enhancement of radiofrequency fields in ferromagnetic materials. In RD-NMR experiments it is necessary to use a radiofrequency field of sufficiently high strength that the transition probability between magnetic sublevels be comparable with the probability of decay of

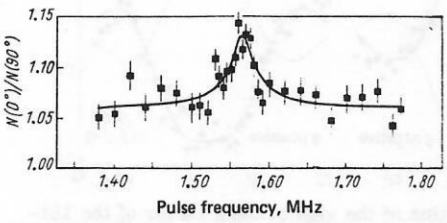

FIG. 19. Stroboscopic quadrupole resonance for the 398-keV state of ^{69}Ge($9/2^+$) in metallic Zn (Ref. 29).

the excited state. This means that the period of precession in the radiofrequency field H_1 must not be greater than the lifetime τ of the nuclear state or

$$H_1 \geqslant \hbar/(g\mu_N \tau). \quad (43)$$

It follows from this equation that for a state with $\tau \approx 1$ msec it is necessary to work with $H_1 \approx 100$ G. For a long time it appeared that it was impossible to produce a radiofrequency field of the power necessary to carry out experiments successfully with short-lived nuclear states. Only in 1965 did it become clear[32] that the amplitude of the radiofrequency field at the nucleus on which the hyperfine structure field H_{hf} is acting in a given ferromagnetic material is increased and its effective value is

$$H_1^{eff} = (1 + H_{hf}/H_0) H_1/2, \quad (44)$$

where H_0 is the strength of the external magnetic field, which in NMR experiments usually reaches several thousand gausses. Therefore to observe NMR of short-lived nuclei implanted in ferromagnetic materials it is sufficient to use a rather low-power radiofrequency field. For radiofrequency detection of NMR in-beam it is possible to use the following methods:

1) Observation of the asymmetry of the β radiation of polarized nuclei (β-NMR-PAD);

2) observation of the anisotropy of the γ radiation of aligned nuclei (γ-NMR-PAD).

The first method was used by Sugimoto[33] in 1966 to measure the magnetic moment of the 20-msec ground state of ^{12}B obtained in the reaction ^{11}B(d,p). The experimental geometry is shown in Fig. 20. Polarized recoil nuclei emitted at 45° to the deuteron beam direction were captured by a metallic foil. The atationary magnetic field H_0 in which the NMR was accomplished preserved the polarization of the nuclei. The capturing foils were selected from materials in which the spin relaxation time was sufficiently long. The asymmetry of the β radiation was measured by means of two semiconductor Si(Li) detectors. At the resonance frequency of the field H_1 the nuclear polarization disappeared, which led to disappearance of the asymmetry of the β radiation. Sugimoto's results, obtained for various stopping foils, are shown in Fig. 21. The error in the final value of the magnetic moment $\mu = 1.003(1)$ nuclear magnetons is due primarily to the Knight shift in the metals used as capturing foils. It cannot be estimated reliably,

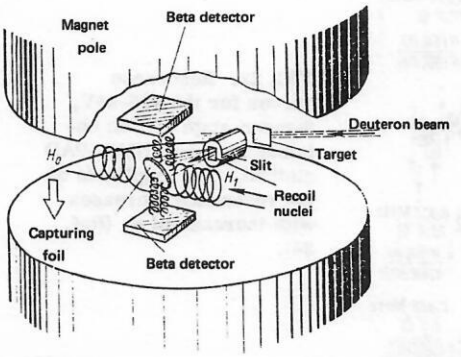

FIG. 20. Diagram of in-beam β-NMR-PAD experiment.[33]

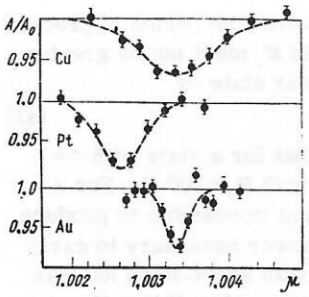

FIG. 21. Resonance determination of the magnetic moment of ^{12}B implanted in various metals.[33] The shift of the resonance curves is due to the Knight shift.

as the result of lack of data on the electronic states of boron in metals.

The method of observing γ-ray anisotropy has been used by Quitmann *et al.*[34] in NMR measurements for the 426-keV isomeric state of ^{73}As with lifetime 8.4 μsec. Aligned ^{73}As nuclei were produced in a target of liquid metallic gallium in the reaction $^{71}Ga(\alpha, 2n)$. The resonance curves obtained in this work for three values of the radiofrequency field H_1 amplitude are shown in Fig. 22. The two-humped shape of the resonance curves is in complete agreement with the theoretical predictions of Matthias *et al.*[35]

The NMR-PAD method has also been used by the Sugimoto group[36] to determine the quadrupole splitting of the ^{12}B magnetic resonance line in a hexagonal single crystal of ZrB_2. If the magnetic dipole interaction is stronger than the electric quadrupole interaction, then two quadrupole splitting lines should appear in the NMR spectrum of ^{12}B with spin $I=1$ (Fig. 23). The central line, which appears at a higher radiofrequency field H_1, corresponds to two-photon transitions. Measurements of the splitting as a function of the angle between the magnetic field direction and the axis $\hat{b}$ of the single crystal permitted the conclusion that the electric field gradient possesses axial symmetry and gave a quadrupole interaction value $|eqQ/h| = (38.7 \pm 1.1)$ kHz. From comparison of this value with the similar quantity for ^{11}B it is possible to find the quadrupole-moment ratio $Q(^{12}B)/Q(^{11}B) = 0.33 \pm 0.03$.

To determine the sign of the magnetic hyperfine interaction in RD-NMR experiments it is possible to use

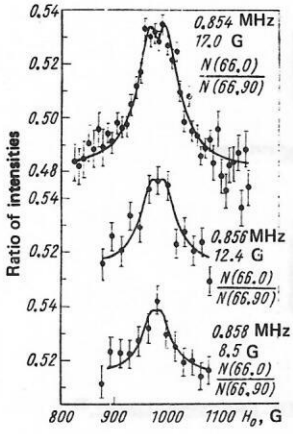

FIG. 22. Resonance curves for the 426-keV, 8-msec state of ^{73}As obtained by the γ-NMR-PAD method. The amplitude of the resonance increases with increase of H_1 (Ref. 34).

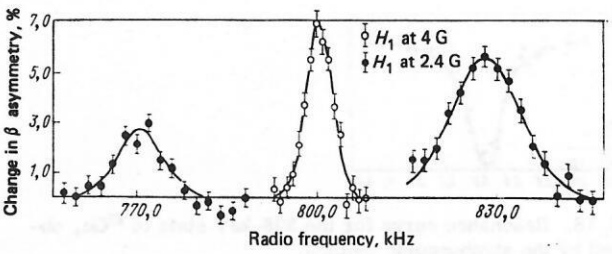

FIG. 23. NMR spectrum for ^{12}B in ZrB_2.

circular polarization of the field H_1, using two pairs of radiofrequency coils.[33] However, it is also possible, as proposed by Matthias *et al.*,[35] to determine the sign of the interaction by fixing the phase of the radiofrequency field with respect to the moment of creation of the excited state of the nucleus being studied. For in-beam work this requires relating the phase of the field H_1 to the beam pulse bombarding the target. Such an experiment has been carried out by Focke *et al.*[37] for the 181-keV, 120-μsec state of ^{78}Br excited in the reaction $^{78}Se(p, n)$. The results of measurements for two phase angles $\Delta = 0$ and 180°, which are shown in Fig. 24, indicate that the sign of the g factor is positive.

The γ-NMR-PAD method in-beam is discussed from all aspects by Riegel *et al.*[38] These authors describe the advantages of the γ-NMR-PAD method over the DPAD and SIPAD methods:

1. For experiments with nonmetals or in recoil into vacuum the longitudinal magnetic field in the γ-NMR-PAD method can play an important role in preserving the nuclear orientation.

2. The shape of the resonance curve in the SIPAD method is very sensitive to instability of the beam pulsing and to deviation of the detector from the ideal location. The latter factors do not affect the resonance curve in the NMR-PAD method with random phases.

3. The NMR-PAD method can be used for measurements of large internal magnetic fields in cases where the DPAD and SIPAD methods are not suitable as the result of limited time resolution.

4. The broadening of the resonance curve due to inhomogeneity of the magnetic field or to small electric field gradients limits the use of the SIPAD method in practice to investigations in solid materials of interaction of nuclei with lifetimes less than 1 msec. The

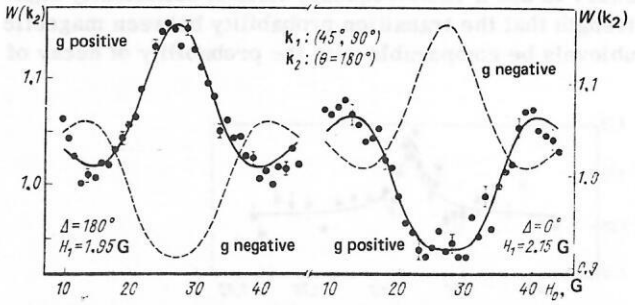

FIG. 24. Determination of the sign of the g factor of the 181-keV, 120-μsec state of ^{78}Br by the fixed-phase method in the γ-NMR-PAD technique.[37]

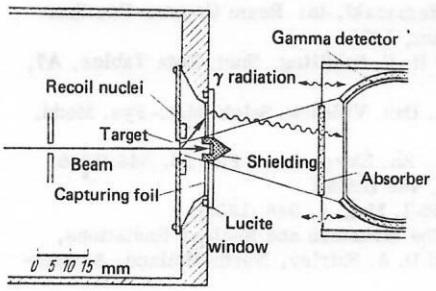

FIG. 25. Apparatus for study of Mössbauer effect for recoil nuclei implanted in the capturing foil.[41]

NMR-PAD method can be used in studies of the interactions of nuclear states with significantly longer lifetimes.

Mössbauer spectroscopy in-beam. Mössbauer spectroscopy in accelerator beams was used for the first time in 1965 by Seyboth *et al.*[39] and Lee *et al.*[40] in studies of Coulomb-excited γ transitions. Since that time Mössbauer experiments for states excited in a Coulomb interaction have been carried out in a number of laboratories. A substantial advance in studies of the Mössbauer effect in-beam is the use of the technique of implanting excited nuclei in various materials[41] (Fig. 25). Excited recoil nuclei emitted from a thin target are stopped in a foil which serves as a source of γ rays in the Mössbauer measurements. In-beam Mössbauer experiments have permitted measurements to be made for the new nuclide ^{73}Ge (Refs. 42 and 43) (Fig. 26), and also for new excited states in ^{160}Gd, ^{164}Dy and ^{168}Er (Ref. 44). In addition, in-beam Mössbauer spectroscopy is a productive method of studying radiation damage and the behavior of impurity atoms in various materials.[45,46]

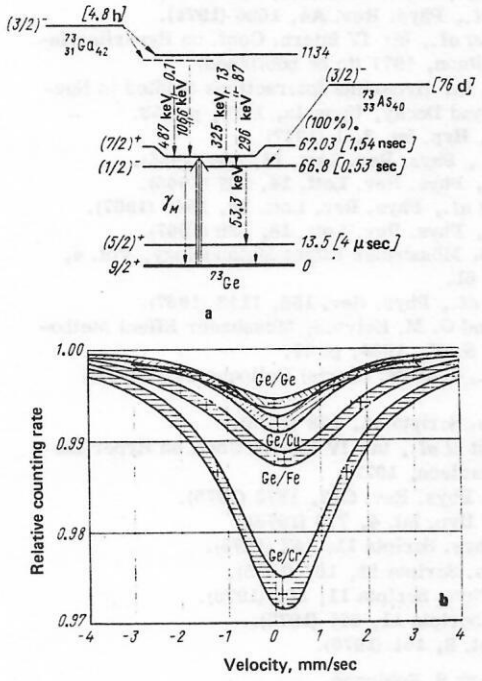

FIG. 26. Level scheme of ^{73}Ge (a) and Mössbauer spectra (b) for the 67.03-keV transition of ^{73}Ge implanted in various materials. The spectra were recorded with an absorber of natural germanium.[43]

4. FIELDS OF APPLICATION OF METHODS OF STUDYING HYPERFINE INTERACTIONS IN-BEAM

Measurement of magnetic dipole and electric quadrupole moments of nuclei. Development of methods of studying hyperfine interactions in accelerator beams has opened new possibilities for measurement of nuclear moments. One can list a number of problems for whose solution precision measurements of nuclear moments can have the highest significance.[47] For example, values of magnetic moments of single-particle states in the region of lead provide information on the modification of the magnetic-moment operator due to the influence of meson exchange on the orbital g factors of the nucleons, and also information on configuration mixing and core polarization.

The g factors of spontaneously fissile isomeric states of odd nuclei serve as a verification of the Nilsson levels in the second potential energy well. Study of the dependence of the g factors of even–even nuclei on the spin of high-spin states of the ground-state rotational band provide information on the nature of backbending.

The determination of the values of electric quadrupole moments of 2^+ states in spherical nuclei, which are close to rotational states, has become one of the reasons for introducing a new seniority scheme[47] with seniority number $\varkappa$. To verify this scheme, it would be of great significance to measure quadrupole moments for the higher-spin states of the ground-state rotational band, and also the Q values of the first 3^+ states in even–even nuclei.

Use of the large magnetic fields of hyperfine structure has significantly extended the possibilities of measuring magnetic moments of states with very short lifetimes. The record measurement is the determination of the g factor $+0.47 \pm 0.09$ of the 2^+ 2.23-MeV state of ^{32}S with a lifetime $\tau = 0.225 \pm 0.020$ psec.[48]

This measurement utilized the transient magnetic field in an iron single crystal acting on ^{32}S recoil nuclei excited in inelastic scattering of α particles. The observed rotation angle of the γ-ray distribution was 1.05 $\pm$ 0.18 mrad.

When use is made of stationary internal magnetic fields which act on nuclear reaction products implanted in ferromagnetic materials, it is necessary to approach with great caution the interpretation of the results of integral measurements. The work of Bozek *et al.*[49,50] has shown that the observed angular displacement of the integral angular distribution of γ rays is in many cases highly underestimated. This effect is evidence that not all implanted nuclei occupy in the crystal lattice of a ferromagnetic material positions at which the total magnetic field is acting. The dependence of the observed effect on the lifetime of the excited states of different isotopes of the same element shows that even the ratio of the g factors of two nuclear states of a given element cannot be determined reliably if they have different lifetimes.

Application of hyperfine interactions in solid-state

studies. During recent years there have been published a number of reviews devoted to investigation of solids by hyperfine-interaction methods,[51-55] and therefore we limit ourselves here to enumerating some of the main directions of research.

1. Measurements of hyperfine magnetic fields and electric field gradients at impurities introduced by implantation into various materials.

Measurements of the internal magnetic fields for impurities of transition d metals are a source of information on the s-d interaction, while those for s-p impurities provide information on the polarization of the conduction electrons. The implantation method has particular advantages in the case of the rare earth elements, since as a result of their large ionic radii they do not dissolve in Fe, Co, or Ni, and in other metals their solubility is negligible.

2. Studies of radiation damage in pure metals, alloys, and dielectrics.

Performance of measurements for different target temperatures and different time scales provides the possibility of investigating not only the nature and stationary distribution of defects, but also studying their dynamics and the evolution of their interactions with implanted impurities.

3. Study of phase transitions.

Measurements near the Curie temperature T_C permit determination of the critical exponent from the relation

$$H_{hf}(T)/H_{hf}(0) = B(1 - T/T_c)^{\beta}.$$

4. Study of the Knight shift.

Precision measurements by the stroboscopic-resonance and NMR methods in-beam determine rather accurately the dependence of the shifts on a number of factors.

Studies of the states of highly ionized atoms. Experiments carried out with recoil ions moving in vacuum or a gas permit investigation of excited states of highly ionized atoms (see the review by Goldring[16]). It turns out that light atoms emitted from targets are in most cases in the ground state, i.e., so-called "cold ionization" has an overwhelming probability. For heavy ions the main role is played by "hot" ionization, which leads to creation of highly ionized atomic states. These states are de-excited through cascades of fast optical transitions, which creates in the nucleus fluctuating magnetic fields. One can hope that further development of these studies will permit investigation of a new region of atomic excitations not accessible for study by other methods.

[1]K. Alder *et al.*, Rev. Mod. Phys. **28**, 432 (1956).
[2]R. M. Diamond *et al.*, Phys. Rev. Lett. **16**, 1205 (1966); **20**, 802 (1968).
[3]J. O. Newton *et al.*, Nucl. Phys. **A95**, 357 (1967).
[4]N. Morinaga and T. Yamazaki, in: Beam Gamma-Ray Spectroscopy, Amsterdam, 1976.
[5]L. C. Northcliffe and R. F. Schilling, Nucl. Data Tables, **A7**, 233 (1970).
[6]J. Lindhard *et al.*, K. Dan. Vidensk. Selsk. Mat.-Fys. Medd. **33**, No. 14 (1963).
[7]B. N. Samoĭlov *et al.*, Zh. Éksp. Teor. Fiz. **36**, 644 (1959) [Sov. Phys. JETP **9**, 448 (1959)].
[8]M. A. Grace *et al.*, Phil. Mag. **4**, 948 (1959).
[9]L. Grodzins, Hyperfine Structure and Nuclear Radiations, eds. E. Matthias and D. A. Shirley, North-Holland, Amsterdam, 1968, p. 607.
[10]J. Lindhard and A. Winther, Nucl. Phys. **A166**, 413 (1971).
[11]M. Forterre *et al.*, Phys. Lett. **B55**, 56 (1975).
[12]J. L. Eberhardt *et al.*, Phys. Lett. **B56**, 329 (1975).
[13]M. B. Goldberg *et al.*, Hyp. Int. **1**, 429 (1976).
[14]M. Hass *et al.*, Phys. Rev. **C14**, 2119 (1976).
[15]J. L. Eberhardt *et al.*, Hyp. Int. **3**, 195 (1977).
[16]G. Goldring, Hyperfine Interactions in Isolated Ions (to be published).
[17]H.-D. Betz, Rev. Mod. Phys. **44**, 465 (1972).
[18]L. Grodzins and O. Klepper, Phys. Rev. **C3**, 1019 (1971).
[19]A. Abragam and R. V. Pound, Phys. Rev. **92**, 943 (1953).
[20]M. Blume, Nucl. Phys. **A167**, 81 (1971).
[21]H. Frauenfelder and R. M. Steffen, in Alpha-, Beta-, and Gamma-Ray Spectroscopy, K. Siegbahn, ed., Vol. 2, Amsterdam, 1965, p. 997.
[22]A. Z. Hrynkiewicz, Postepy Fiz. **11**, 521 (1960).
[23]A. Iordachescu *et al.*, Phys. Lett. **B48**, 28 (1974).
[24]H. Haas *et al.*, Phys. Rev. Lett. **30**, 656 (1973).
[25]R. E. Horstman *et al.*, Phys. Lett. **B48**, 31 (1974).
[26]B. Haas *et al.*, Nucl. Phys. **A194**, 249 (1972).
[27]J. Christiansen *et al.*, Phys. Rev. Lett. **21**, 554 (1968).
[28]J. Bosse and H. Gabriel, in: Hyperfine Interactions Studied in Nuclear Reactions and Decay, Uppsala, 1974, p. 262.
[29]G. Schatz *et al.*, in: Hyperfine Interactions Studied in Nuclear Reactions and Decay, Uppsala, 1974, p. 264.
[30]M. Deutsch and S. C. Brown, Phys. Rev. **85**, 1047 (1952).
[31]D. Connor, Phys. Rev. Lett. **3**, 429 (1959).
[32]A. M. Portis and R. H. Linqvist, Magnetism, Vol. **11A**, N. Y., 1965.
[33]K. Sugimoto, Hyperfine Structure and Nuclear Radiations, Amsterdam, 1968, p. 859.
[34]D. Quitmann *et al.*, Phys. Lett. **B30**, 329 (1969).
[35]E. Matthias *et al.*, Phys. Rev. **A4**, 1626 (1971).
[36]T. Minamisono *et al.*, in: IV Intern. Conf. on Hyperfine Interactions, Madison, 1977 (to be published).
[37]B. Focke *et al.*, in: Hyperfine Interactions Studied in Nuclear Reactions and Decay, Uppsala, 1974, p. 258.
[38]D. Riegel *et al.*, Hyp. Int. **3**, 1 (1977).
[39]D. Seyboth *et al.*, Phys. Rev. Lett. **14**, 954 (1965).
[40]Y. K. Lee *et al.*, Phys. Rev. Lett. **14**, 957 (1965).
[41]G. D. Sprouse *et al.*, Phys. Rev. Lett. **18**, 1041 (1967).
[42]G. Czjzek *et al.*, Phys. Rev. Lett. **18**, 529 (1967).
[43]F. E. Obenshein, Mössbauer Effect Methodology, Vol. 4, N. Y., 1968, p. 61.
[44]R. S. Stevens *et al.*, Phys. Rev. **158**, 1118 (1967).
[45]G. D. Sprouse and G. M. Kalvius, Mössbauer Effect Methodology, Vol. 4, N. Y., 1968, p. 37.
[46]D. Seyboth *et al.*, J. Phys. (Paris) Colloque **35**, C6-305 (1974).
[47]K. Kumar, Phys. Scripta **11**, 179 (1975).
[48]J. A. G. de Raedt *et al.*, in: IV Intern. Conf. on Hyperfine Interactions, Madison, 1977.
[49]E. Bożek *et al.*, Phys. Rev. **C12**, 1873 (1975).
[50]E. Bożek *et al.*, Hyp. Int. **4**, 773 (1978).
[51]H. de Waard, Phys. Scripta **11**, 157 (1975).
[52]H. Bernas, Phys. Scripta **11**, 167 (1975).
[53]E. Recknagel, Phys. Scripta **11**, 208 (1975).
[54]H. Haas, Phys. Scripta **11**, 221 (1975).
[55]G. Vogl, Hyp. Int. **2**, 151 (1976).

Translated by Clark S. Robinson